Design, Modeling and Evaluation of a 2.4GHz FHSS Communications System for *NarcisSat*

Kyle Doerksen, Jean-Francois Levesque, Ignacio Mas

Advisor: Robert Twiggs
Space Systems Development Lab
Stanford University, Stanford, CA, USA 94305

1. Abstract

Communication subsystems generally consume the majority of power and a significant fraction of mass and volume for picosatellites, and thus their design is critical to the overall satellite and mission plans. The available data bandwidth defines the types of payloads that can be accommodated. Until now, most CubeSat designs have used the 2m (145MHz) and 70cm (437MHz) bands. We present simulation and experimental measurements of a commercial, off-the-shelf (COTS) spread spectrum 2.4GHz system that is incorporated on *NarcisSat*, a CubeSat scheduled for launch in late 2003. In the 2.4GHz band, patch antennas instead of monopoles are suitable, eliminating the need to deploy antennas on orbit. With the system presented here, data rates of up to 115kbps are possible, facilitating new kinds of more data intensive payloads than previously possible in CubeSats. Spread spectrum is well suited for multiple CubeSat deployment and handles ground-based noise better than narrowband communications. We also address the attitude control subsystem and ground station requirements of this system.

2. Introduction

2.1. CubeSat overview

The CubeSat program was started in 1999 to facilitate access to space for universities that are building picosatellites by standardizing launch integration using the P-POD launcher. The flight-certified P-POD launcher can accommodate three CubeSats and may be easily integrated as a secondary payload on many types of launches. By standardizing size and mass requirements ($10\times 10\times 10$cm cube, 1kg), the collaborative initiative by California Polytechnic University and the Space Systems Development Lab at Stanford has encouraged dozens of international teams to develop satellites in this common CubeSat form factor [1,2,3].

2.2. *NarcisSat* overview

The NarcisSat project began in winter of 2001 with a series of space systems engineering classes taught at Stanford by CubeSat originator Robert Twiggs. From three preliminary designs the best features were combined into one model and hardware development began in spring of 2002. The key mission objectives are the operation of a COTS *Sanyo VPC-X360* digital camera, and the proof of concept of a 2.4GHz frequency hopping spread spectrum communication system that is described in this paper. The spacecraft will be launched in Low-Earth Orbit (*LEO*) at an altitude yet to be determined, but likely over 600km. For optimal visibility (communication link occurrence and duration), our simulations show that a 60° inclination orbit at 900km altitude is most desirable.

3. Requirements

The communications subsystem of NarcisSat had several design requirements. Most generally, the communications system is required to receive commands from the ground, and transmit data back (digital photographs and telemetry). Small size (no dimension larger than 10cm), and mass (<100g) were important to fit in the CubeSat envelope. Also important were low power consumption (<1W average, partial Tx duty cycle), appropriate EIRP (~1W), and the highest possible data rate (>9600 baud) since photos are 85kB to 200kB depending on the quality setting. The radio must accommodate Doppler shifts up to 10kHz and withstand environmental stresses of the launch and space environment. We sought a frequency band for which a variety of COTS parts and a suitable ground station were available. Finally, the communications system needed to integrate with the *Z-World* (Davis, CA) Z-180 based microprocessor of the C&DH subsystem via RS-232, and interface with an external antenna that provides adequate gain and coverage for successful operation.

4. Radio

The radio chosen was a *MicroHard Corp* (Calgary, AB) *MHX-2400* OEM 2.4GHz, frequency hopping spread spectrum radio, marketed for unlicensed use in the 2.4000 - 2.4835 GHz ISM band. It has a mass of approximately 75g, an industrial temperature rating from -40 to +70°C, sensitivity of -108 dBm, features an MCX antenna connector, 16 bit CRC with

optional forward error correction, CPFSK modulation, adjustable RF power from 10mW to 1W and is completely controllable over a single RS-232 port. While there are a plethora of 2.4GHz ISM band RS-232 products, the *MHX-2400* is one of the most compact and sensitive, well documented and suited for our application.

The MHX-2400 has a fixed bit rate of 115200 baud, but it may be interfaced with serial ports speeds of 2400 to 115200 bps. In practice this means that if a link can be established, data rates of 115200bps are possible. However, NarcisSat's data transmission speed as is limited by the Z-World Z-180 CPU serial I/O performance. This radio does not allow reduction of bit rate to increase link margin.

In earlier trade studies we considered the *Kenwood TH-D7* and *Alinco DJ-C5T* HAM transceivers, which have been employed in several other picosatellite designs. The Kenwood has an incorporated terminal node controller (*TNC*), but this TNC is unreliable and limited in functionality. The *Yaesu* requires an external TNC that consumes additional mass, volume and power. The MHX-2400 incorporates packetization and control functionality and RF components onto a single, compact board, making it ideal for our application. While it can operate within the 2390-2450 MHz HAM band it does not feature station ID, so an FCC waiver is required for our ground station.

The MHX-2400 has master and slave modes, the difference being that the master can remotely set the radio parameters of connected slave units. In our configuration, the master is at the ground station and the radio on the satellite configured as a slave.

4.1. Spread spectrum

By spreading RF energy across a range of frequencies, spread spectrum techniques improve a communication system's noise rejection capabilities. Two basic techniques exist: frequency hopping spread spectrum (FHSS) and direct sequence spread spectrum (DSSS). The FHSS technique works by transmitting a series of narrowband bursts, where the center frequency of that transmission changes every few milliseconds, while DSSS works by spreading RF energy continuously over a wide bandwidth.

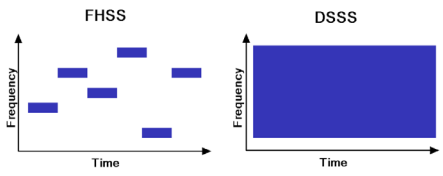

Figure 1 *FHSS vs. DSSS bandwidth utilization*

One advantage of spread spectrum for CubeSats is the ability to communicate with and between multiple nearby CubeSats operating in the same frequency band, since it may be compelling to launch several CubeSats together on a single launch. Also, selection of hopping patterns makes it possible to avoid narrowband interference from RF devices near the ground station.

4.2. Power Consumption

Table 1 *MHX- 2400 Power Consumption*

	Mean Power Consumption (W)				
Output Power	**1W**	**500mW**	**250mW**	**100mW**	**10mW**
Stand By	0.89	0.89	0.89	0.89	0.89
Receiving	1.12	1.08	1.04	1.02	0.99
Transmitting	1.37	1.22	1.17	1.12	1.07
Beacon Mode	1.94	1.69	1.52	1.32	1.23

5. Antennas

In order to reduce the complexity of the attitude control system, an isotropic radiating pattern is often desirable for small satellites. With that initial goal in mind, we evaluated two kinds of antennas for the NarcisSat communication system: monopoles and patch antennas.

5.1. Monopole antennas

Since wavelengths at 2.45GHz are 12cm, a ¼λ-monopole is only 3cm long and can be stowed on one edge or face of a CubeSat. However, it still needs to be deployed. The radiation pattern for a monopole is donut-shaped around the antenna, with a gain generally less than 2dB and almost no power transmitted along the antenna axis. Monopole antennas are a good solution for quasi-isotropic transmission when the spacecraft is tumbling in space. The 'blind zone' at the end of the antenna is about 20° wide and it must not point at the ground station to achieve a link.

When a monopole is oriented perpendicular to a face of the cube, the cube reflects radiation. This considerably reduces the radiation power on the other side. As a result, a monopole on each side of the cube must be considered, using an RF splitter to feed the two antennas at a cost of some power losses, and additional mass and volume in the structure. Other drawbacks of having more than one antenna are the necessity of stubs and precise feed-cable lengths to match the impedances at a rather small wavelength in order to avoid signal reflection and loss of efficiency.

When using more than one antenna, the antenna pattern is a function of both the geometric

arrangement of the antennas and the phase of the signal fed to each one. For instance, two monopoles placed end-to-end will produce a different pattern if the signal is differentially phased between the feed lines. If the two signals are phased 180° to each other, a single-lobe donut will result from the constructive interference (because the geometry is also phased 180°); if the two signals are in phase, destructive interference will occur and no signal will result from the antenna array.

In the NarcisSat case, if two monopoles are placed on opposite faces of the cube, we have the complex situation where the geometric distance between the antennas is on the order of the wavelength. This produces a set of radiation lobes and nulls, the signal phase only changing the location of the lobes (Figure 2), never leading to homogeneity. This antenna pattern is not suitable for our application because some minor satellite rotations would result in loss of contact. Adding additional monopoles around the cube to limit the radiation gaps makes the analysis more complex but does not solve the problem.

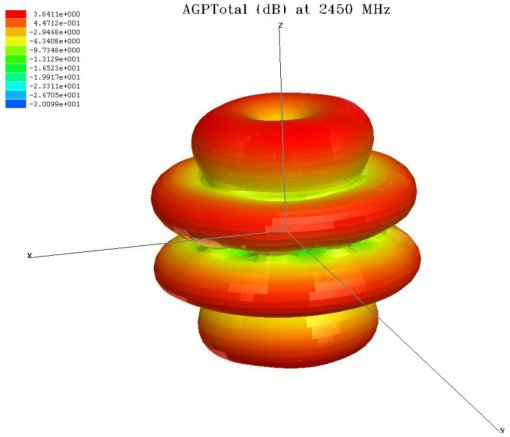

Figure 2 *Interference pattern of two monopoles*

In addition, antenna polarization might also be a problem when using monopole antennas. Monopole antennas radiate only linearly (E-field parallel to the antenna), and the spacecraft is tumbling. If the ground station cannot receive both vertical and horizontal components of a radiation source, the link might be rendered unusable. Crossed or circular-polarized antennas would be a better solution.

5.2. Patch antenna

Patch antennas are a suitable alternative to monopoles when using microwave frequencies. They consist of two parallel conductive plates having their resonant frequency in their operating frequency band. By using dielectric material between the plates, the dimensions can be significantly reduced. No deployment is required for patch antennas since they are thin and can be integrated with the CubeSat face.

Patch antenna radiation is perpendicular to the plane of the antenna and has a hemispherical shape, often right or left-hand circularly polarized. The gain varies according to the design but is generally about 6 to 10dB along the radiation axis, giving a reasonable beam width of 60° to 120°. To get a communication link, the patch must point the ground station, making the pointing requirements more demanding than for a monopole.

Combination of two or more patch antennas is possible but complex to model and phase appropriately. When using two patches on opposite faces, each patch radiates approximately a hemisphere, but there is a deep RF null around the equator of the arrangement. At any given time, one lobe points to the ground station, and the other off to deep space. The transceiver's 1 watt is split into these two lobes, so the Earth side sees only 0.5W EIRP. Also, some RF energy goes opposite the desired directivity of each patch (Figure 4), destructively interfering with the other patch's pattern and reducing the benefit of the two-patch antenna solution. For more than two patches, the complex radiation interference pattern can only be evaluated through simulations or measurements. We modeled several configurations, with various phasing configurations, and none solved the isotropy or RF-splitting problems. Adding more elements only creates more interference patterns that in 3-D cannot perfectly superimpose on each other in a constructive manner; there will always be constructive and destructive regions of the interference pattern making the radiation not isotropic. As a practical concern, each patch consumes surface area of NarcisSat, displacing solar cells and reducing the amount of power available for transmission and other tasks.

For NarcisSat we have selected a 3× 5cm circularly-polarized patch antenna from *GRE America* (Belmont, CA). The single patch antenna offers many advantages over monopoles: robustness and circular polarization, with no RF-splitting or deployment. Since, the radiation is not isotropic, we need some kind of attitude stabilization, but the pointing requirements on the AD&C subsystem design can be met with a simple system.

5.3. Antenna Simulation

In order to arrive at the antenna design, radiation patterns were simulated using *Ansoft HFSS* software

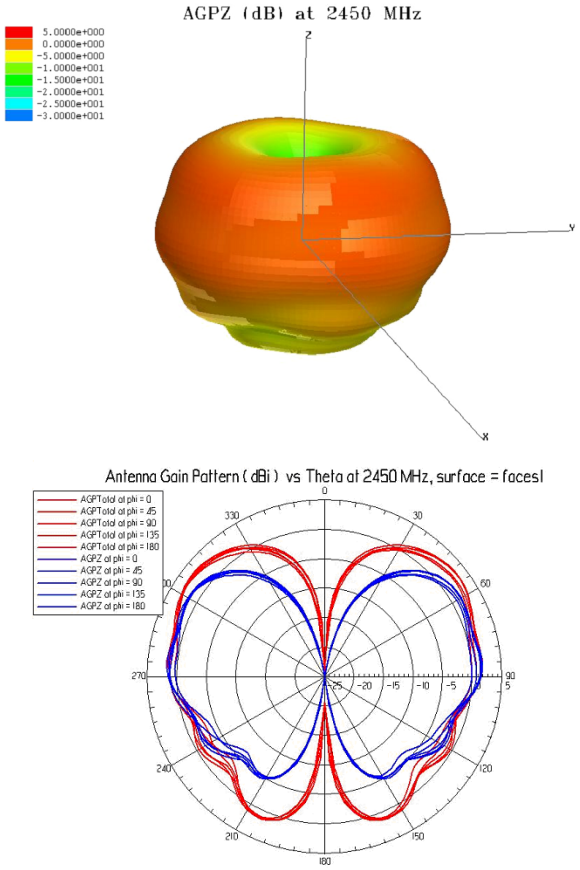

Figure 3 *Monopole antenna radiation pattern*

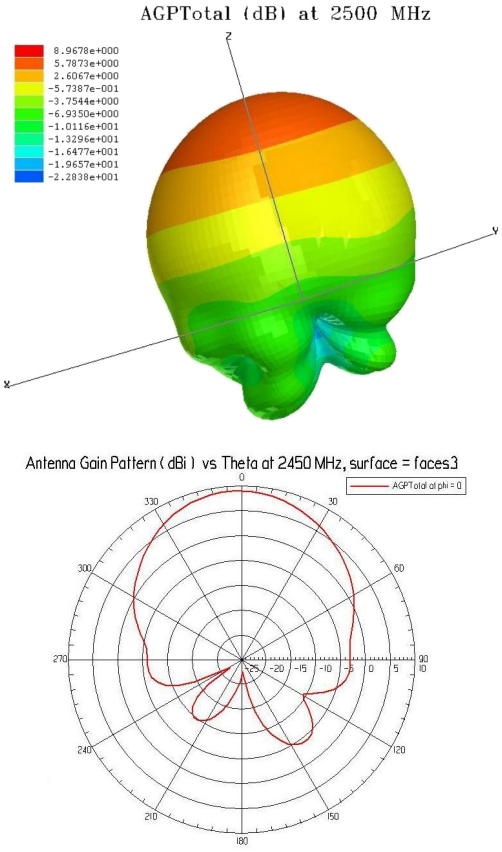

Figure 4 *Patch antenna radiation pattern*

(Pittsburgh, PA). Among all the options and antenna combinations analyzed, only two designs were suitable for our application: one featuring a single monopole and one a single patch antenna.

For the monopole simulation, a 3.1cm copper conductor has been inserted on the face of a 10cm aluminum cube. The simulation uses a perfectly matched layer (*PML*) as the radiation interface around the model. Running the simulation for a 1W source at 2.45GHz gives us the results shown in Figure 3.

As seen on the figure, the pattern is a donut shape with less power radiated toward the face of the cube because of reflection.

For reasons explained above, a patch antenna from GRE America was chosen for our design. A model of the patch antenna has been simulated using HFSS. The model consists of two copper plates separated by 2mm of *Teflon* dielectric. Dimensions were measured from the real GRE patch antenna.

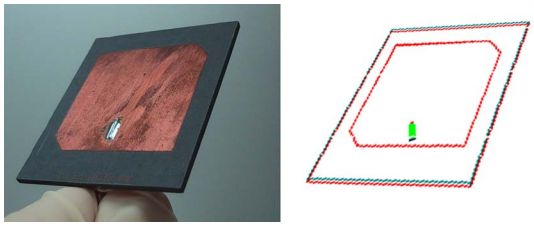

Figure 5 *GRE Patch antenna and HFSS model*

In the simulation, the antenna is mounted on a 10cm × 10cm × 15cm[1] aluminum structure. The feed line has been modeled and connects under the patch antenna. The simulation results (Figure 4) show a hemispherical pattern, which agrees with the expected and manufacturer's indicated specifications. The beam width is approximately 60° with acceptable side lobes. Experiments confirmed this result by measuring signal strength a fixed distance away from a rotating 10cm × 10cm × 15cm aluminum cube with an attached GRE patch antenna and 2.4GHz transmitter.

[1] Originally from a "cube and a half" satellite design, but effectively identical to a standard CubeSat for this RF model.

6. AD&CS

Because of the directionality of the single patch antenna pattern, an attitude determination & control subsystem is necessary to keep the communication antennas in an appropriate orientation to successfully communicate. Based on the antenna pattern above and the link budget (Table 2), we find that NarcisSat must point to within ±60° in order to close the communication link.

We considered passive stabilization and active control for NarcisSat. A passive system does not require power, attitude determination or control laws, but sacrifices considerably flexibility. To meet our requirements of simplicity, robustness and power consumption, and satisfy our relatively basic pointing requirement, passive magnetic stabilization is used.

6.1. Stabilization using permanent magnets

Permanent magnets are the most straightforward way to make the spacecraft align with the Earth's magnetic field lines. However, since the orientation of the field lines varies greatly with respect to the spacecraft's magnetic latitude, this technique limits communication opportunities to ground stations located in a small latitude range. For instance, a configuration in which the antenna points to a ground station located at 50°N latitude cannot be used in the southern hemisphere where it will point the antenna off into space.

A model for the torque T_{MAG} produced from a permanent magnet in a magnetic field is described as:

$$T_{MAG} = M_{MAG} \times B_0 \sin\theta \tag{1}$$

θ is the angle between the magnet's magnetic moment M_{MAG} and the Earth's magnetic field B_0 at the satellite's position in space. Derived from Gauss's law for bars [4], the magnets' magnetic moment M_{MAG} is given by its magnetic induction B_{MAG} for a given material of volume V_{MAG}.

$$M_{MAG} = \frac{B_{MAG} V_{MAG}}{\mu_0} \tag{2}$$

μ_0 is the permittivity of vacuum. This model assumes a perfect distribution of the magnet's field lines surrounding the magnets and the spacecraft.

6.2. Damping and Hysteresis model (2-D)

Without damping, NarcisSat would spin and oscillate indefinitely about the magnetic field lines with amplitudes ranging as high as ±180°. Magnetic hysteresis materials are used to dissipate the tumbling energy and damp the oscillations. In such materials, kinetic energy is transformed into heat due to friction in realigning magnetic domains in response to time-varying external magnetic fields.

Hysteresis materials essentially act as magnets, but their residual magnetic flux density (or magnetic induction) B_{HYST} will change and reverse in response to the component of the local field intensity H_0 in the direction of the hysteresis material's magnetic domains [5]. This component is denoted H_τ and is used for the B-H hysteresis diagram below (Figure 6).

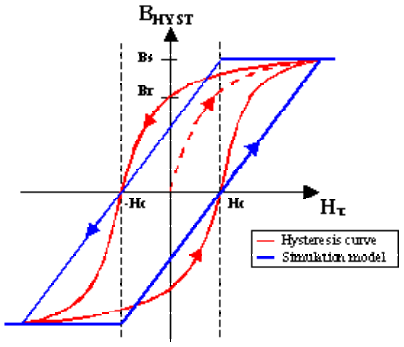

Figure 6 *Magnetic hysteresis model*

Energy dissipation can be computed from the area of the hysteresis diagram of the material used. In all case, the field threshold must be lower than the field applied ($H_C << H_\tau$) in order to overcome the friction and produce a boundary change into the material. The local field intensity component H_τ is given by the Earth's magnetic induction B_0 as:

$$H_\tau = \frac{B_0}{\mu_0} \sin\phi \tag{3}$$

φ is the angle between the Earth's magnetic field lines and the hysteresis bars' magnetic domains. The Earth's magnetic induction B_0 can be computed for any magnetic latitude and altitude of the spacecraft on its orbit using known equations [6]. The local field direction must also be calculated using the L-shell model equation relative to the magnetic North. As for the permanent magnet, the dynamic equation for the hysteresis bar is then:

$$T_{HYST} = M_{HYST} \times B_0 \sin\phi \tag{4}$$

6.3. System dynamics

To achieve maximum damping in the underdamped system, the hysteresis material should be oriented perpendicularly to the magnetic field lines and permanent magnets (making $\varphi=\theta+90°$). When combining the permanent magnets and hysteresis rods, the system's dynamics, for a spacecraft with a moment of inertia I_S, is given as:

$$I_S\ddot{\theta} = T_{MAG} + T_{HYST} = M_{MAG} \times B_0 \sin\theta + M_{HYST} \times B_0 \cos\theta \quad (5)$$

This system appears to be non-linear even when excluding the hysteresis. Furthermore, on the hysteresis side, when the oscillation amplitude gets lower, the angle φ doesn't allow H_τ to overcome the threshold H_C. Thus, no further boundary changes occur and no more energy gets dissipated from the oscillations. At first glance, it may seem to be the critical point where the oscillations are minimum. But, since the hysteresis bars are acting as magnets, the dual-component system has its resulting magnetic dipole tilted off the desired axis, which was intended to be along the permanent magnets. This new axis is not fixed and flips over with the change of polarity inside the hysteresis bars. With the smoothing of the oscillations, the induction on the material gets lower and lower until the polarity ceases to get reversed. The resulting magnetic dipole axis is then fixed and no more energy dissipation will occur from magnetic boundary displacement inside the hysteresis material. The system is no longer damped and a quiescent oscillation will remain. Therefore, the minimum oscillation amplitude is determined by the resulting magnetic dipole angle of the permanent magnets and hysteresis bars.

Since the magnetic moment is given by the material's volume and its magnetic induction, for given material properties, a mass tradeoff can be achieved in order to reduce the final oscillation amplitude. This accuracy θ_C can be approximated, when neglecting the polarization threshold H_C, by the following equation:

$$\theta_C = \arctan\left(\frac{B_S V_{HYST}}{B_{MAG} V_{MAG}}\right) = \arctan\left(\frac{B_S \rho_{MAG}}{B_{MAG} \rho_{HYST}} \times \frac{m_{HYST}}{m_{MAG}}\right) \quad (6)$$

B_S is the saturation magnetic induction of the hysteresis material and ρ and m are respectively the density and mass of the materials. The polarization threshold H_C at low-Earth orbit contributes only for few degrees on this critical angle and has been neglected to simplify the equation.

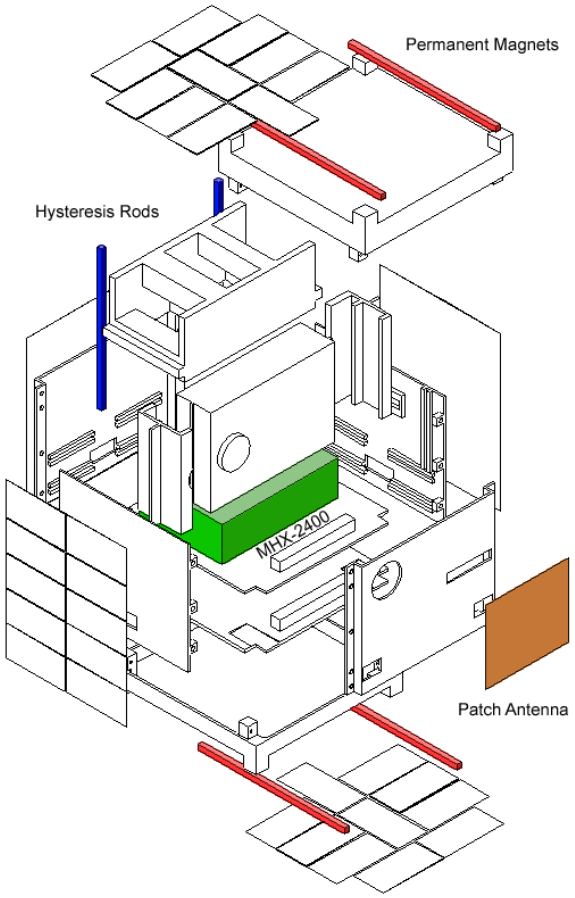

Figure 7 *NarcisSat exploded view. The two hysteresis rods behind the antenna face have been removed for clarity.*

6.4. AD&CS Simulation

According to the model explained earlier, a tradeoff between hysteresis bars and permanent magnet has to be made. In our design, we use four bars (28g) of strong magnet material (*Alnico-5 Br=1.28 Tesla*) aligned with the patch antenna in order to point to the ground station located at about 37°N latitude. Perpendicular to the magnets are two bars (17g) of hysteresis material (*Carpenter HyMu-80, B_S=0.73 Tesla, Br=0.35 Tesla, Hc=1.0 A/m*).

We simulated a 1kg/10cm cube with the mentioned magnets and hysteresis rods in a 60°-inclination low-Earth orbit using *Simulink*. Hysteresis was modeled using delay, slope and saturation. The simulation uses the previous equations of motion with 180° of initial field angle error (worst case).

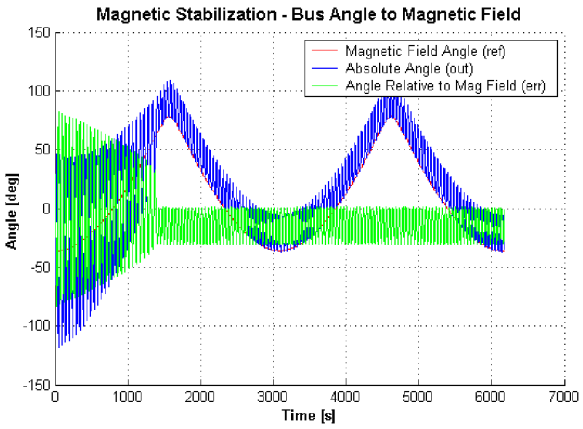

Figure 8 *Passive magnetic stabilization simulation results for one orbit*

The results show a damped oscillation for 22 minutes about the Earth's magnetic field lines before a critical point is reached where the system's response tends to oscillate about the magnetic field line with relatively low amplitude. This effect demonstrates the magnetic behavior of the hysteresis rods when the polarization is no longer periodically reversed. Then, the system is stable and closely follows the Earth's magnetic field lines. The 30° of quiescent oscillation also confirms the previous theory.

Note that the simulation is planar and does not include gyroscopic precessions around field lines or spins of the spacecraft. It does, however, take into account these motions as input parameters to the computation. A more accurate simulation model is being developed to include gyroscopic effects as well as to compute the system's response in 3-D.

6.5. Experimental measurements

In order to get an accurate description of our system, we have measured the actual magnetic moments of NarcisSat's bar magnets and hysteresis rods in a Helmholtz coil. Different setups of field strength have been used on a hanging magnet oscillating in the field. For the permanent magnets in bars of $3.68 \times 3.68 \times 100$mm, the mean measured magnetic moment is 8.6 A/m^2. This result assumes a linearly oscillating system.

7. Ground Station

Because the path loss is much greater at 2.4GHz than 437MHz much more ground gain is required. For the NarcisSat ground station we are using a 20m-diameter dish operated by SRI. This dish has recently been retrofitted for solid-state motion control and is located in the foothills behind Stanford. At 2.4GHz the dish has a calculated gain of 51dB with f/D=0.42.

Figure 9 *20m ground station antenna (SRI. Palo Alto, CA)*

7.1. Feed horn

To operate at 2.4GHz we have designed, simulated, fabricated and tuned an appropriate 2.4GHz choked circular waveguide feed horn. Simulation helped to confirm our feed horn design parameters, estimate feed horn gain, and adjust feed probe length and choke ring position to achieve the optimal antenna pattern (Figure 11).

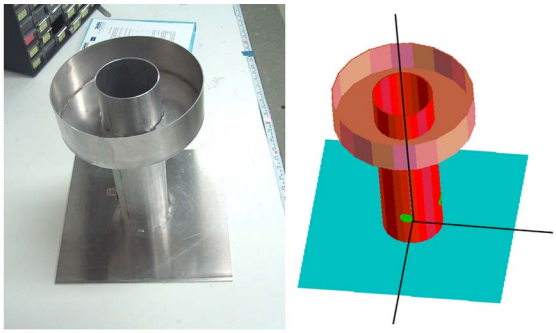

Figure 10 *2.4GHz cylindrical waveguide feed horn*

With two feed probes arranged at right angles to each other, the feed may be circularly polarized using a 3dB hybrid coupler, or may be operated in linearly polarized mode using only one feed probe.

An MHX-2400 identical to the one on NarcisSat is located in a weatherized box mounted on the feed platform, near the feed horn to minimize cable loss. The RS-232 interface of the MHX-2400 is converted

to RS-485, which uses differential signaling to support cable runs up to 4000ft, and connected to the ground station PC in the building below the dish (visible in Figure 9).

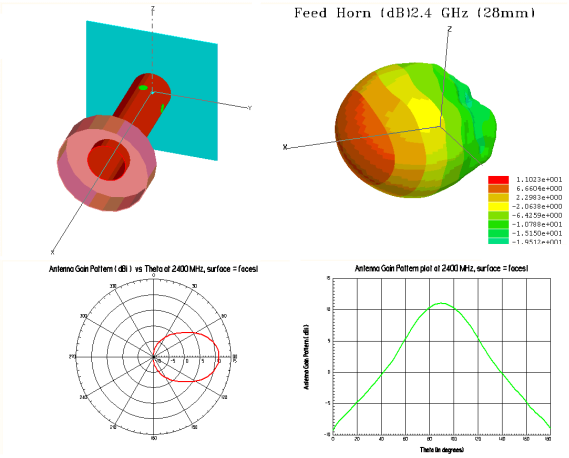

Figure 11 *Feedhorn simulation in HFSS*

8. Operational Simulation

8.1. Ground patterns and ground station visibility

In order to get an estimate of the spacecraft visibility by the ground station we have developed a custom simulator using the Keplerian equations and *Matlab* (Figure 12). This software allows us to easily compute the ground trace and ground station tracking information for different orbit parameters. The simulation results shown in this section assume a 900km circular orbit with 60° inclination. The simulation has been run many times over one full day and for 3 possible ground station locations (Stanford (PA), New York (NY) and Würzburg, Germany (WU)), each with a minimum antenna elevation of 5° in all directions.

Approximately seven consecutive ground passes out of 14 orbits occur each day for each ground station. At 900km altitude, the passes last 11 minutes on average for Stanford.

Other simulation results show optimal satellite visibility occurs at 60° orbit inclination. At 50°, only 6 ground passes per day and at 600km, the average duration is reduced to 9 minutes. Also, for a polar orbit, the passes are no longer consecutive.

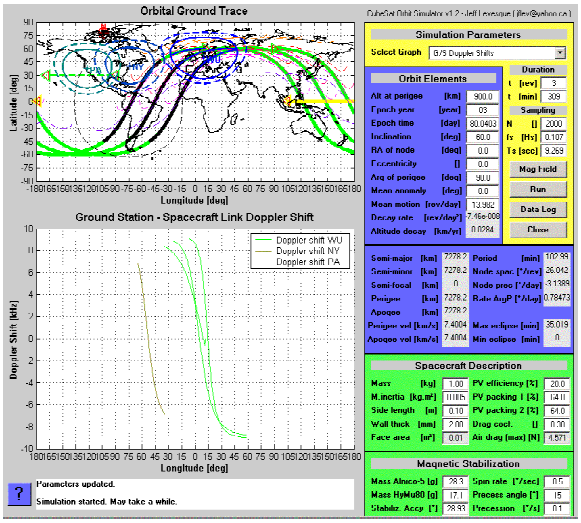

Figure 12 *CubeSat orbit simulation interface*

8.2. Doppler shift

Because the Doppler shift for space operations is considerably higher than for most ground-based applications we tested the MHX-2400 for its robustness in high Doppler shift conditions. Using the *Matlab* orbital simulation, maximum Doppler shifts were calculated. With the same orbital parameters as above, the Doppler shift curves for one day for three potential ground station locations are shown in Figure 13.

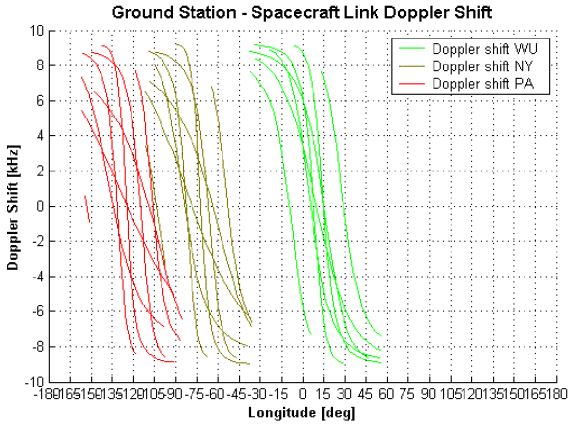

Figure 13 *Doppler shift simulation for one day - 60° inclination, 900km circular orbit*

The maximum frequency shift is 9.1kHz and a frequency shift rate of 70Hz/s for any of the 3 ground stations. For a lower altitude orbit (600km), the Doppler shift raises to 10kHz.

To simulate the Doppler shift with the MHX-2400 hardware, we used the setup shown in Figure 14.

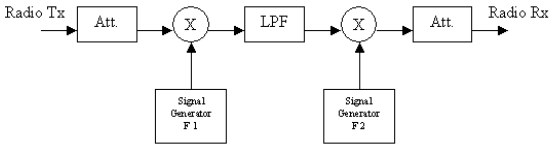

Figure 14 ***Doppler shift test setup***

The transmitted radio signal goes through an attenuator to protect the mixer, and is mixed with F1 (F1 and F2 are approximately 2.4GHz). The low-pass filter (LPF) removes the high frequency components and the low frequency is mixed with F2. The result goes to the receiver through the second attenuator, which is adjusted so that the total attenuation from Tx to Rx equals the calculated net path loss of the satellite link. The frequency received at the receiver (Rx) is F= 2.4GHz + (F2 – F1). When (F2 – F1) is equal to 10kHz the maximum Doppler Shift conditions are simulated.

We tested Doppler shifts up to 50kHz and packet loss was less than 1% even in these extreme conditions, thus the MHX-2400 exceeds the Doppler requirement.

8.3. Link budget

A link budget has been computed using the methods described in SMAD [6] (Table 2). The ground station used is a 20m dish antenna with appropriate feed horn. On the spacecraft, a single patch antenna, which we modeled above, is assumed to be pointing at the ground station within ±30°. The transmission power both on the ground and on-board is 1W (determined by the MHX-2400 transceiver), hence the ground-space and space-ground link budgets are the same. A 900km orbit is used to compute the slant range of approximately 3000km with 5° minimum ground station elevation due to mountains on the horizon near the SRI antenna. From the SMAD equations and tables, the antenna gains, and the receiver sensitivity, we compute a link margin of 21dB, which is more than sufficient to operate NarcisSat. With the very high ground station gain, the ground station pointing accuracy is critical. Pointing errors >0.5° will reduce the link margin to zero. The link budget shows that a smaller dish may be better since it will give sufficient margin with less sensitivity to pointing errors.

Table 2 *Link Budget (following SMAD 13-13)*

Item	Symbol	Unit	Value
Frequency	f	MHz	2400.0
Transmitter Power	P	W	1.0
Transmitter Power	P	dBm	30.0
Transmitter Line Loss	L_l	dB	-1.0
Transmit Antenna Beamwidth	θ_t	deg	60.0
Peak Transmit Antenna Gain	G_{pt}	dBi	8.7
Transmit Antenna Pointing Error	e_t	deg	30.0
Transmit Antenna Pointing Loss	$L_{\theta t}$	dB	-3.0
Equiv. Isotropic Radiated Power	**EIRP**	**dBm**	**34.7**
Propagation Path Length	S	km	3000.0
Space Loss	L_s	**dB**	**-169.6**
Propagation and Polarization loss	L_{pp}	dB	-0.6
Receive Antenna Diameter	D_r	m	20.0
Min elevation	ε_{min}	deg	5.0
Receive Antenna Beamwidth	θ_r	deg	0.4
Peak Receive Antenna Gain	G_{rp}	dBi	51.5
Receive Antenna Pointing Error	e_r	deg	0.1
Receive Antenna Pointing Loss	$L_{\theta r}$	dB	-0.6
Net Receive Antnena Gain	G_{rn}	**dBi**	**50.9**
Sensitivity	***Sens***	**dBm**	**-108.0**
Inplementation Loss	L_i	dB	-2.0
Margin	**M**	**dB**	**21.42**

9. Future work

9.1. Alternative network topologies

The MHX-2400 can operate in repeater mode, allowing for more complex communication networks. Repeaters pass information along to other repeaters/slaves, but also act as slaves in that they pass data to/from their serial port. This could be useful for CubeSat applications in which the repeater node could communicate with the ground at the maximum power setting, while other satellites flying in close formation could communicate with the ground via the repeater and operate at a reduced power level. By using spread spectrum, the same frequency band can be shared by several satellites, without retuning antennas, etc.

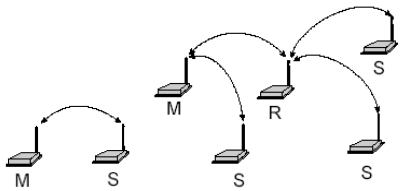

Figure 15 ***Master-Slave (left) and Master-Repeater-Slave (right) network topologies***

After successful operation with the 20m dish, the link budget presented in Table 2 suggests that 5-7m ground station dishes may also be able to achieve a link with margins of 10-12dB. This would make 2.4GHz communication systems accessible to many CubeSat teams, and it might be possible to tie several such ground stations together into a network.

As presented by Cutler et al [7], using multiple ground stations together as a virtual ground station controlled over the Internet is an effective method of increasing total contact duration per orbit, and therefore bringing more data back from picosatellites. Our dynamics simulations indicate that several northern hemisphere stations will be flown over with suitable antenna pointing.

Once NarcisSat is launched we can use telemetry data to confirm the 3-D satellite dynamics models (with magnetic stabilization and hysteresis) that we are developing. Current measurements from the solar panels on each side of the cube can be used to reconstruct the satellite's rotation. Measurements from the ground station can be used to evaluate packet loss and data throughput to determine the suitability of this communication system design for other picosatellite designs.

10. Conclusions

In this paper we have presented the design for a 2.4GHz communications system for NarcisSat. Spread spectrum has several advantages, and 2.4GHz opens up new antenna possibilities such as patch antennas, which we have modeled, tested and included in the design of NarcisSat.

The selection of radio and antenna eliminated the often overlooked power, mass and volume needs of an external TNC, and the mass, volume and design difficulties of splitting, matching networks and antenna phasing which are required with most designs. Tests and simulations indicate that this communication system meets the Doppler, link and other requirements, while being almost entirely COTS.

With this design, pointing is necessary because only a single patch antenna is used. However, this pointing accuracy can be achieved using simple passive magnetic stabilization with bar magnets and hysteresis rods. Our simulations indicate that the satellite will stabilize shortly after launch and follow the Earth's field lines to within the required pointing accuracy for the duration of the mission.

The satellite dynamics and ground trace simulation software written in Matlab can be easily extended and applied to other picosatellite projects.

The 2.4GHz communications system presented here is scheduled to be flown on NarcisSat in autumn 2003. If it is as successful as our simulations lead us to hope, it may be a very promising alternative to the 70cm and 2m systems currently used. The approach presented here, of detailed RF and communications simulation can be adapted to other CubeSat programs around the world.

11. Acknowledgements

Robert Twiggs, director of the Space Systems Development Lab has been perpetually supportive of new ideas and approaches to space projects. Our RF mentors Lars Karlsson and John Ellis have given their knowledge and equipment with RF testing and simulation. Yoann Duriaud has helped with simulation and measurements, as has Brett Allard. The entire NarcisSat team led by Mike Colonno has worked together to make NarcisSat a reality. We would also like to acknowledge Mike Cousins at SRI who so graciously lets us use the SRI Palo Alto high gain antenna facility for our ground station.

12. References

1. Heidt, H., Puig-Suari, J., Moore, A.S., Nakasuka, S., Twiggs, R.J., "CubeSat: A New Generation of Picosatellite for Education and Industry Low-Cost Space Experimentation," Proceedings of the Utah State University Small Satellite Conference, Logan, UT, August 2001, pp. 1-2, 6.
2. Nason, I., Creedon, M., Puig-Suari, J., "CubeSat Design Specifications Document," Revision V, Nov. 2001, pp. 1-6. <http://ssdl.stanford.edu/cubesat>.
3. Nason, I., Puig-Suari, J., Twiggs, R.J., "Development of a Family of Picosatellite Deployers Based on the CubeSat Standard," Proceedings of the IEEE Conference, Big Sky Montana, IEEE, 2002.
4. *Electromagnetic Induction*. Reed College Physics. <http://academic.reed.edu/physics/courses/Phys100/lab18/faraday.pdf>
5. Kelly, J., "Analysis of Hysteresis for Attitude Control of a Microsatellite," San José State University.
6. Wertz, J.R. Larson, W.J., *Space Mission Analysis and Design*, Microcosm & W.J.Larson, 3rd Edition, 1999.
7. Cutler, J. W., Fox, A., Bhasin, K. Applying the Lessons of Internet Services to Space Systems. *IEEE Aerospace Conference*, Big Sky, Montana, March 9-16, 2002